

Received July 9, 2019, accepted July 31, 2019, date of publication August 5, 2019, date of current version August 19, 2019.

Digital Object Identifier 10.1109/ACCESS.2019.2933010

Binary Particle Swarm Optimization for Scheduling MG Integrated Virtual Power Plant Toward Energy Saving

M. A. HANNAN¹, (Senior Member, IEEE), M. G. M. ABDOLRASOL², M. FAISAL¹,
P. J. KER¹, (Member, IEEE), R. A. BEGUM³, AND A. HUSSAIN¹

¹Department of Electrical Power Engineering, College of Engineering, Universiti Tenaga Nasional, Kajang 43000, Malaysia

²Centre for Integrated Systems Engineering and Advanced Technologies, Universiti Kebangsaan Malaysia, Bangi 43600, Malaysia

³Center for Water Cycle, Marine Environment and Disaster Management (CWMD), Kumamoto University, Kumamoto 860-8555, Japan

Corresponding author: M. A. Hannan (hannan@uniten.edu.my)

This work was supported in part by the Ministry of Higher Education under the Universiti Tenaga Nasional, Malaysia, under Grant 20190101LRGS, and in part by the Universiti Tenaga Nasional Bold Strategic under Grant 10436494/B/2019093.

ABSTRACT This paper introduces a novel optimal schedule controller to manage renewable energy resources (RESs) in virtual power plant (VPP) using binary particle swarm optimization (BPSO) algorithm. It is crucial to minimize the costs giving priority for sustainable resources use instead of purchasing from the national grid. The effectiveness of the proposed approach is examined by the IEEE 14 bus system containing microgrids (MGs) integrated with RESs in the form of VPP. Real load demand recorded is used to model and simulate the test case studies of the system for 24 h in Perlis, Malaysia. Moreover, weather data collected from the Malaysian Meteorological Department such as wind, solar, fuel, and battery status data are used in the BPSO to find the best ON and OFF schedules. The results found that the developed BPSO algorithm is robust in reducing energy consumption and emissions of the VPP. This study contributes to the development of an optimization algorithm for an optimal scheduling controller of MG integrated VPP in order to reduce carbon emissions and manage sustainable energy. Finally, a comparative analysis of the optimal algorithms over conventional justifies the use of RESs integration and validates the developed BPSO for sustainable energy management and emissions reduction.

INDEX TERMS Virtual power plant, microgrid, energy management, carbon reduction, scheduling controller, optimization.

I. INTRODUCTION

Empirical research on global warming and climate change identifies the CO₂ emission as the key factor for increasing the atmospheric GHG emissions [1]. Climate change threatens the quality of life and the habitability of planet earth for many species, which significantly reduce the prospect of ensuring energy, environmental sustainability, and economic effectiveness (3E) of energy supply. Therefore, energy efficiency and renewable sources have become the focus of GHG emission reduction efforts to the researchers. Study shows that, in Malaysia, 85% of total electricity is harvested through fossil fuel. Therefore, CO₂ will continue to increase since the electricity demand is expected to increase by 4.2%

The associate editor coordinating the review of this manuscript and approving it for publication was Taufik Abrao.

per year till 2040. Thus, generating electricity from renewable sources increased remarkably from 2012 to 2017, and expected to increase by 11% of the total generated power in 2020 [6], [7]. Afterward, Long-range Energy Alternatives Planning (LEAP) System was devised to monitor the CO₂ emission for fossil fuel-based industrial sector [8]. Though, some achievements have been observed regarding the control of CO₂ emissions, however, a huge gap still now exists between the energy target and energy efficiency. Therefore, workable effective mitigation policies need to be introduced to reduce the CO₂ emission and thus improve sustainable economic development. Fig. 1 reflects the per capita CO₂ emission starting from 2005 to present and is projected till the year 2020 and Fig. 2 gives the change of fuel combustion in the same period [9]. From the figures, it is clear that per capita CO₂ emission in Malaysia is expected to reach at 9.5 metric

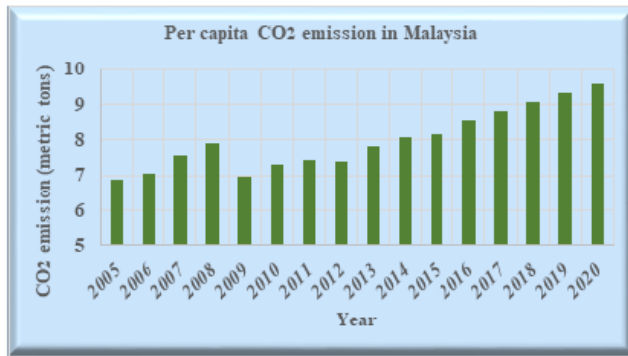


FIGURE 1. Per capita CO₂ emission from 2005 to 2020 in Malaysia.

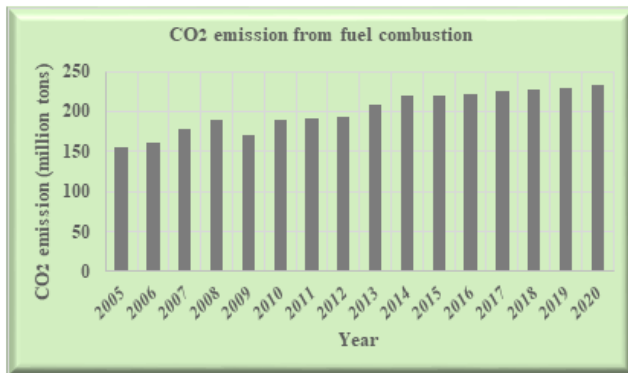


FIGURE 2. Fuel consumption starting from 2005 to 2020 in Malaysia.

tons in 2020 with the increased fuel combustions of about 225 million tons in the same year.

Microgrid (MG) is a small-scale power system consists of the cluster of controllable thermal or electrical loads, energy storage system (ESS) and distributed sources operating together with isolated or grid-connected mode [10], [11]. MG is the key aspect to increase the reliability, stability and reduce the energy losses, reactive power support for voltage profile improvement, GHG emission and consumption [12] by controlling the volatility and intermittency of the power sources. However, costs, protection, efficiency, and control issues are still a great concern of MG technology. Against this backdrop, virtual power plant (VPP) is a novel concept mainly rely on information technologies (IT) develop for sustainable energy utilization. VPP can be modeled to operate for local distributed sources or can provide ancillary services for centralized renewable plants. Therefore, the relationship between VPP and MG integrated with RES has been focused on energy management system (EMS) to perform the decision-making strategies considering the load forecasting and monitoring of market demand analysis.

Previous research on EMS shows that MG based VPP depends on the islanded or stand-alone and grid-connected operation. In Island or stand-alone mode, a multiplatform control device such as DSP is used in developing EMS controllers for the standalone system consists of PV and diesel

integrated with ESS [13], [14]. However, in grid-connected mode, MG operates as a current controller to inject power to the national grid or store the surplus power to supply whenever it is required, depending on the available power, load demand and unit price [15], [16]. In [18], suitable scheduling considering the interactions between aggregators, market operators, system operators, generators, and consumers has been proposed to reduce the uncertainty associated with the stakeholders. Uncertainty of wind turbines has been considered in day-ahead scheduling of the virtual power plant to manage the energy and reserve electricity market [19]. However, a simple demand-side model is presented in this paper. Other researches on EMS focuses on the fuzzy logic controller technique; however, these techniques need huge optimization data and trial-and-error procedures for setting the control parameters [20]. Therefore, researchers still now focus on developing the improved VPP towards energy saving and emission reduction for future MG implementation.

Recently, optimization techniques have been widely used to improve and optimize the performance by minimizing the overall costs and saves the energy, considering the factors associated with the system. Artificial intelligence controller and genetic algorithm are analyzed to ensure the system stability and smooth transition of MG considering the peak load shaving in grid-connected and standalone mode [21]. A multi-agent decentralized EMS based distributed intelligence is designed for optimal carbon-energy combined-flow (OCECF) of a combined large-scale power system [22]. However, the notable drawbacks of the artificial intelligent technique are the high investment and replacement costs and requirement of the enormous amount of data for setting the control parameters. Therefore, researches do not rely on this controller to predict the operation of each source to ensure accuracy, reliability and to minimize the cost. Significant aspects of MG connected VPP are pointed as increased network efficiency and security, reduction of cost and emission, supply the required amount of energy and controlling the peak shaving [23].

Optimization techniques such as PSO [24], genetic algorithm (GA) [21], gravitational search algorithm (GSA) [25], lightning search algorithm (LSA) [26], Quantum-behaved lightning search algorithm (QLSA) [27] are used as the improved technique to solve the traditional issues of the existing technology. However, these algorithms have the limitation of complex parameter calculation and formulation, coding difficulties and longer computational time in finding the best fitness value. In some applications, it has been observed that-battery integration is discouraged and intermittency of distributed sources are not considered [28]. Study shows that binary optimization is very helpful in searching optimal dispatch, unit commitment problems and dynamic multi-objective functions in MG operation under uncertainty conditions [29].

Scheduling is a set the data in the form of ON and OFF of the MG sources based on demand and sustainable power utilization [30]. However, ON and OFF of MG sources need to

be optimized in order to minimize power consumption [31]. Previously, symbiotic organisms search algorithm and dolphin echolocation optimization have been used in MG operation to find an optimal schedule of ON and OFF of MG sources [32]. However, the objection function in minimizing the cost of the MG sources and reducing the emissions are not priorities in the above optimization. In this paper, binary PSO algorithm has been used to search for the optimal schedule for EMS dealing VPP integrating RES sources for 24 hours using IEEE 144 bus test system. Binary PSO (BPSO) is advantageous for simple calculation, easy handling, high convergence rate and minimum storage requirement. 100 iterations are performed to find the best schedule to reach the target objective of minimizing the power and reduce CO₂ from the main grid.

II. OVERVIEW OF VPP AND MG RELATIONS

A VPP is a multi-technology unit, which contains both renewable and non-renewable sources integrated with energy storage systems connected with smart devices and information communication systems [33], [34]. VPP is a cloud-based distributed power plant that coordinates the heterogeneous distributed energy resources (DERs) to increase the power generation, as well as trading or selling power on the open market [35]. The motivation behind creating VPP technology is to coordinate the various types of energy resources to minimize the cost of power generation and maximize the profits received from the sale of that power. A MG refers to a small-scale power system with a cluster of loads and distributed generators operating together through energy management systems. However, MG is a cluster of local DERs and loads which operates within the grid either in grid-connected or stand-alone mode at a low or medium voltage level.

The concept of VPP integrated with MG's RES merging is a holistic manner to combine their strengths for improving efficient energy utilization [36]–[38]. However, their strength and weakness have not been thoroughly investigated in different applications. For example, a single MG is too small to participate in electricity markets. However, a VPP model consists of multiple MG could significantly improve the profitability in electricity trade-off [39]. Therefore, this paper emphasis on overcoming the aforementioned shortcomings in the existing VPP model. Thus, the significant outcome from this study assists the utilities enormously in scaling up the implementation and interconnection of DG into existing networks. The notable contribution of this study is the development of optimization algorithm in controlling the power exchange among the interconnected system in order to:

- Reduce the expense of generating electricity, purchase energy from the grid and energy storage cost.
- Develop sustainable energy management system between VPP and MG integrated with RESs.
- Obtain minimum operational cost with the best VPP scheduling to maintain stable and quality power supply to the loads.

- Increase the reliability in the system to gain customer satisfaction.
- Reducing the power losses caused by constraints into DGs, loads, the power-flow, and system operation.
- Achieve the objective of reducing CO₂ emission.

III. VPP AND MG SYSTEM MODELLING

The main system is a standard IEEE Fourteen Bus System representing distribution structures in which the loads in each bus and the distribution impedance are real and actual data. In this study, five MG is included to share the feed loads in each specific bus. The individual MG is modeled with five sources. Detail analysis of the IEEE 14 bus system, load distribution and MG development along with the EMS are illustrated as follows;

A. IEEE 14 BUS STANDARD SYSTEM

A modified IEEE 14 bus system consists of five MG sources and loads has been depicted in Fig. 3, which considered the only one generator at bus 1 to control the grid, while original system contains two generators. Each of the five MG consists of diesel generator, photovoltaic, wind turbine, fuel cell and battery. Although in the standard bus networking system, per unit value is widely used, throughout this study, actual values are considered to find the actual power values for controlling purposes. The main grid is connected to bus1 and supply 200MW of power to the whole system in which the main sub-station transformer converts voltage from 33kV to 11kV at 50Hz of frequency. Five MGs have been installed in the system in different bus bars to enhance system reliability, power quality and to reduce the transmission line losses. Study on the IEEE standard system 1547 reveals that, multiple MG system has the improved operational characteristics to make the system stable and reliable compared to the single MG system [40]–[42].

Each MG supplies 10 MW to the chosen bus bar and the capacity of the bus can cover the supplies in order to avoid tripping during the stand-alone mode of operation. MGs have been installed in bus 5, bus 6, bus 10, bus 11 and bus 13 as in Fig. 3. All the MGs are of the same size with an equal number of sources and each bus of this system is connected to one or multiple buses to develop the entire architecture.

Table 1 shows the impedance of R , X_L , X_C for IEEE fourteen bus test system.

The system contains nine loads located at bus 2, bus 3, bus 4, bus 5, bus 6 and following the bus 9 to bus 14, respectively. Every bus represents a feeder to a specific loading area demand. A real-time load demand curve of Perlis, Malaysia, has been represented in Appendix, which was recorded on February 2016. Maximum peak of each load is shown in Table 2.

B. DEVELOPMENT OF MG SYSTEM

Single line diagram of the interconnected sources has been shown in Fig. 4. The total capacity of each MG is 10MW operated with 415V at 50 Hz. The MG is linked to the

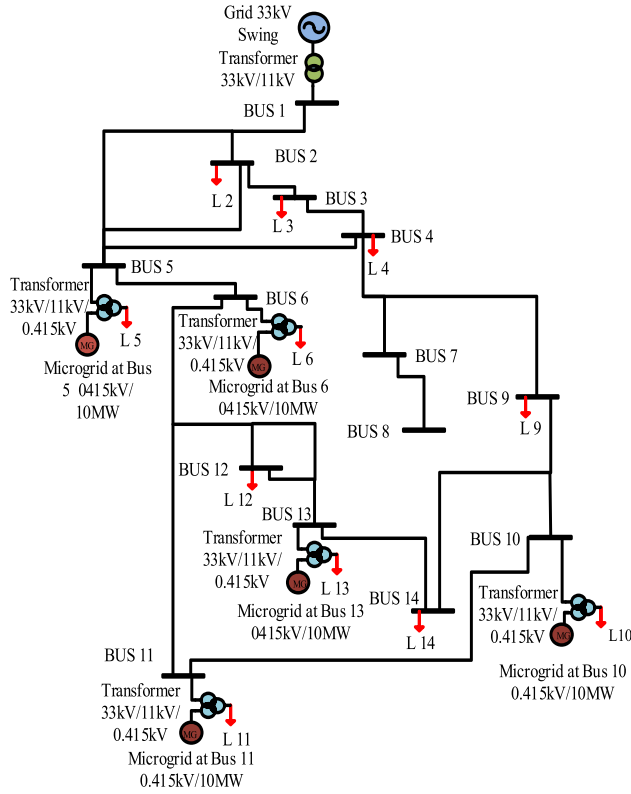


FIGURE 3. Modified IEEE 14 bus system.

TABLE 1. Bus to bus impedance for IEEE 14 bus system.

Bus-Bus	R Ω	X _L Ω	X _C Ω
1-2	0.0234498	0.0715957	0.063880
1-5	0.0653763	0.2698784	0.071632
2-3	0.0568579	0.2395437	0.052998
2-4	0.0703131	0.2133472	0.045254
2-5	0.0689095	0.2103948	0.041140
3-4	0.0810821	0.2069463	0.041866
4-5	0.0161535	0.0509531	0.015488
4-7	0	0.2530352	0
4-9	0	0.1331121	0
5-6	0	0.3049442	0
6-11	0.1149258	0.2406690	0
6-12	0.1487211	0.3095301	0
6-13	0.0800415	0.1576267	0
7-8	0	0.2131415	0
7-9	0	0.1331121	0
9-10	0.0384901	0.1022450	0
9-14	0.1538031	0.3271598	0
10-11	0.0992805	0.2324047	0
12-13	0.2673132	0.2418548	0
13-14	0.2068253	0.4211042	0

distribution bus through a star connected three winding transformer. Each source is connected to AC bus through either DC to AC or AC to AC converters. Table 3 shows the type of distributed generator, its capacity and fuel used. Each source

TABLE 2. Maximum active and reactive power in each bus load in IEEE fourteen bus system.

Bus	P (MW)	Q (MVAR)
1	No Load	No Load
2	15.29507	10.27344
3	68.03108	18.244215
4	35.13784	-0.683445
5	5.4860295	1.51510208
6	7.8513428	5.99371266
7	No Load	No Load
8	No Load	No Load
9	20.8230156	13.47983
10	6.31940556	4.6505054
11	2.47821826	1.475337
12	4.38893102	1.44703688
13	9.61070106	4.854701
14	10.6709611	4.33310932

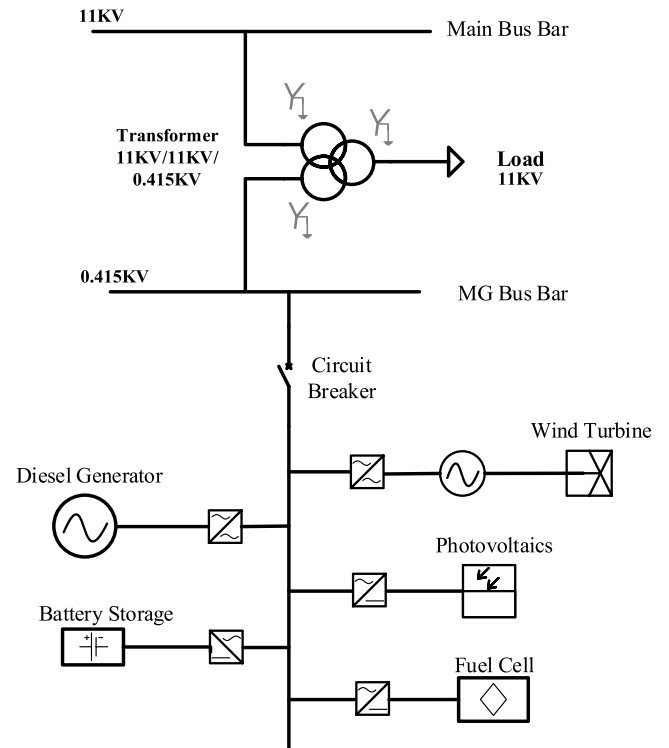


FIGURE 4. Single line diagram of proposed interconnected MG system.

TABLE 3. Microgrid sources characteristics.

Source Type	Capacity	Fuel
Diesel generator	4 MW	Diesel
Photovoltaic (PV)	2 MW	Solar Irradiance
Wind turbine (WT)	2 MW	Wind speed
Solid oxide fuel cell (SOFC)	1 MW	H ₂
Energy Storage System	1 MW	Charging

participates in the VPP based on the controller decision. The scheduling controller decision is generated using PSO optimization algorithm. Parameters of the optimization are weather, loading capacity, battery status, fuel and per unit price.

From the table, solar irradiance and wind speed have been considered for the photovoltaic and wind power respectively. This research has been conducted with the real hourly average weather data, provided by Tenaga Nasional Berhad Research (TNBR), Malaysia. The data tracker records the data of solar irradiance and wind speed in a year and then averaged into an accurate daily reading as depicted in Fig. 5. Another RES, solid oxide fuel cell (SOFC) is used oxide electrolyte to conduct negative oxygen ions from the cathode to the anode to generate electricity and hot water.

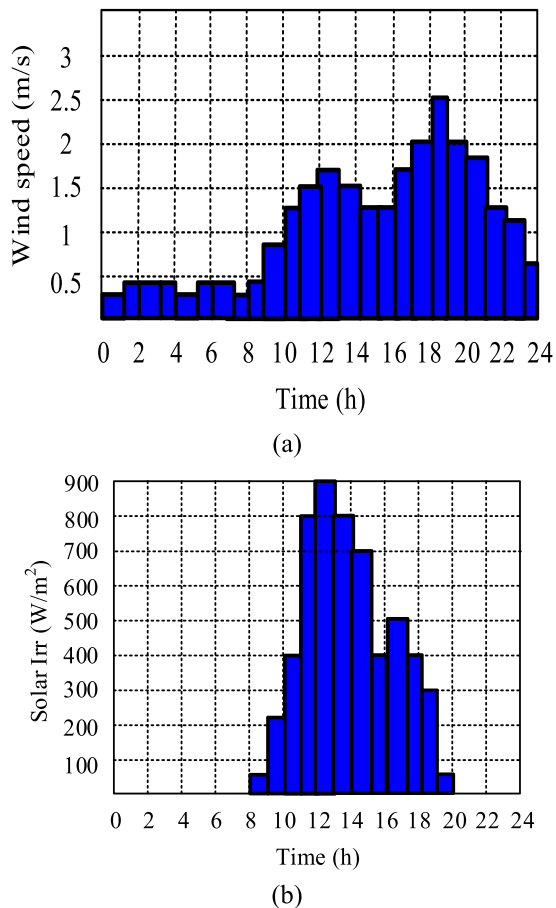


FIGURE 5. a) Real wind speed reading b) Real solar irradiance reading.

IV. OPTIMIZED SCHEDULING CONTROLLER FOR ENERGY MANAGEMENT

Scheduling controller is used to regulating each source in the VPP system for the optimal EMS. In this section, details of BPSO are described to perform the optimal EMS.

A. ENERGY MANAGEMENT SYSTEM

An EMS is a set of transmitters, sensors, data acquisition, data control and data processing systems at distributed generator location. The EMS has a supervisory controller to tasks the scheduling ON and OFF, and resetting temperature set points based on conditions [43]. The main tasks for EMS are to generate suitable set points in smart power sharing among

the sources to economically optimized power dispatch and fulfill specific load demand. Since the irradiance and wind speed are intermittent in nature, therefore, forecasting and fast online algorithms are very important for EMS to define energy availability and the optimized power dispatch signals to the loads. In this research, a novel online BPSO algorithm has been proposed to obtain the minimum operational cost with the best VPP scheduling, maintaining the stable and quality power supply to the loads. Fig. 6 shows EMS of the VPP integrated MG using the BPSO algorithm to the control power flow of the aggregating system.

B. BINARY PARTICLE SWARM OPTIMIZATION ALGORITHM

PSO is a simple concept and computational algorithm which is effectively applied to optimize various continuous non-linear functions [44]. In PSO algorithm, the population is initiated randomly with particles and evaluated to compute fitness function together with finding the particle best (best value of each individual) and global best (best particle in the whole swarm). Initially, with the fixed dimensions and fitness value, each individual determines its particle best. The best individual among the particle best population, on the other hand, the global best is determined and the loop starts to converge to an optimum solution. In the loop, particle and global bests are determined to update the velocity and the current position of each particle. Evaluation is again performed to compute the fitness of the particles in the swarm. This loop is terminated with a stopping criterion predetermined in advance.

The PSO algorithm is simulated with some modifications to generate binary code known as BPSO to control the multi-sources in each MG of the system. However, in the conventional trial and error process, it is impossible to obtain the best schedule for the system. Thus, proposed BPSO is used to control the efficient power supply from the main grid and price using the sustainable resources to save the fuel and the cost. Stepwise BPSO algorithm development has been explained below. To develop this algorithm, twenty swarm has been selected and each swarm representing a cell (Schedule). Thus, the schedule concurrently forms 24 rows \times 25 columns matrix considering the initial condition to make the random cell and a binary cell.

1) INITIALIZATION

PSO algorithm randomly initiates the particles at the beginning to calculate the fitness to get the best value of each individual schedule in the whole swarm. Table 4 shows the pseudo code for the initialization step. BPSO parameters are chosen as the 33kV grid, solar irradiance and wind speed as shown in Fig. 5, and average energy pricing of 43.7 cent/kWh. Firstly, each individual cell with its dimensions and fitness value is assigned to the particle best; however, the best population cell with its dimension and fitness value is, on the other hand, assigned to the global best. Then a loop starts to converge to an optimum schedule by determining the particle

BPSO Scheduling Algorithm																											
Input data	Energy Management System (EMS)																								1 st hour decision		
		1	2	3	4	5	6	7	8	9	10	11	12	13	14	15	16	17	18	19	20	21	22	23		24	
Grid data	S1	0	1	1	0	1	0	1	0	1	0	1	0	0	1	0	0	0	1	0	1	0	1	0	1	DG1 OFF	
	S2	1	0	1	0	1	0	1	0	1	0	0	1	0	0	1	1	1	0	1	0	0	1	0	1	DG2 ON	
	S3	0	1	1	1	0	0	1	0	1	1	0	0	0	1	0	1	1	0	0	0	1	1	1	1	DG3 OFF	
	S4	0	1	0	1	0	1	0	1	0	1	0	0	0	1	0	0	1	1	1	1	1	1	1	0	1	DG4 OFF
Weather Data	S5	0	1	0	1	1	0	1	0	1	0	1	0	0	0	0	1	1	0	1	0	1	1	0	1	DG5 OFF	
	S6	0	1	1	0	1	0	1	0	1	0	1	0	0	1	0	0	0	1	0	1	0	1	0	1	DG6 OFF	
	S7	1	0	1	0	1	0	1	0	1	0	0	1	0	0	1	1	0	0	1	0	0	1	0	1	DG7 ON	
	S8	0	1	1	1	0	0	1	0	1	1	0	0	0	1	0	1	1	0	0	0	1	1	1	1	DG8 OFF	
	S9	0	1	0	1	0	1	0	1	0	0	0	0	1	0	0	1	1	1	1	1	1	1	0	1	DG9 OFF	
	S10	0	1	0	1	1	0	1	0	1	0	1	0	0	0	0	1	1	0	1	0	1	1	0	1	DG10 OFF	
	S11	0	1	1	0	1	0	1	0	1	0	1	0	1	0	0	1	0	0	1	0	1	0	1	0	1	DG11 OFF
	S12	1	0	1	0	1	0	1	0	1	0	1	0	0	1	0	1	1	0	0	1	0	0	1	0	1	DG12 ON
	S13	0	1	1	1	0	0	1	0	1	1	0	0	0	0	1	0	1	1	0	0	0	1	1	1	1	DG13 OFF
	S14	0	1	0	1	0	1	0	1	0	0	0	0	1	0	0	1	1	1	1	1	1	1	0	1	0	DG14 OFF
	S15	0	1	0	1	1	0	1	0	1	0	1	0	0	0	0	1	1	0	1	0	1	1	0	1	DG15 OFF	
Energy Price	S16	0	1	1	0	1	0	1	0	1	0	1	0	0	1	0	0	0	1	0	1	0	1	0	1	DG16 OFF	
	S17	1	0	1	0	1	0	1	0	1	0	0	1	0	0	1	1	0	0	1	0	0	1	0	1	DG17 ON	
	S18	0	1	1	1	0	0	1	0	1	1	0	0	0	1	0	1	1	0	0	0	1	1	1	1	DG18 OFF	
	S19	0	1	0	1	0	1	0	1	0	0	0	0	1	0	0	1	1	1	1	1	1	1	0	1	DG19 OFF	
	S20	0	1	0	1	1	0	1	0	1	0	1	0	0	0	1	1	0	1	0	1	1	0	1	0	1	DG20 OFF
	S21	0	1	1	0	1	0	1	0	1	0	1	0	0	1	0	0	1	0	1	0	1	0	1	0	1	DG21 OFF
	S22	1	0	1	0	1	0	1	0	1	0	0	1	0	0	1	1	0	0	1	0	0	1	0	1	DG22 ON	
	S23	0	1	1	1	0	0	1	0	1	1	0	0	0	1	0	1	1	0	0	0	1	1	1	1	DG23 OFF	
	S24	0	1	0	1	0	1	0	1	0	0	0	0	1	0	0	1	1	1	1	1	1	1	0	1	DG24 OFF	
	S25	0	1	0	1	1	0	1	0	1	0	1	0	0	0	0	1	1	0	1	0	1	1	0	1	DG25 OFF	
Battery																											

FIGURE 6. Block diagram represents BPSO schedule controller operation.

TABLE 4. Pseudo Code For BPSO initialization.

```

Input: X (Schedule matrix)l, I (maximum number of iteration), N
(Swarm size), C1, C2 and w (fixed values) h (No. of hours), s (No. of
status), G (gird power status) R (solar irradiance) W (wind speed), E
(Energy price)
Output: Pbest, minimum Evaluation, MC (fitness function),
for k from 1 to N do
    swarm(h,s) = rand(h,s)
    for i from 1 to h do
        for j from 1 to s do
            if swarm(i,j) > 0.5 then
                swarm_B(i,j)=1 else swarm_B(i,j)=0 end
            end
        end
    end
end
    
```

and global bests to update the velocity. Then the current position of each particle is updated with the current velocity. Evaluation is again performed to compute the fitness of the particles in the swarm under weather conditions and battery status. Creating a random schedule in decimal and converted to binary to be the first test schedule as in Eq. 1 and Eq. 2.

$$swarm_{(h,s)} = rand. \begin{bmatrix} swarm_{(1,1)} & \cdots & swarm_{(1,s)} \\ \vdots & \ddots & \vdots \\ swarm_{(h,1)} & \cdots & swarm_{(h,s)} \end{bmatrix} \quad (1)$$

$$swarmB_{(h,s)} = rand. \begin{bmatrix} swarmB_{(1,1)} & \cdots & swarmB_{(1,s)} \\ \vdots & \ddots & \vdots \\ swarmB_{(h,1)} & \cdots & swarmB_{(h,s)} \end{bmatrix} \quad (2)$$

where, *swarm* and *swarmB* denote the random decimal population matrix and random population binary matrix respectively; *h* = 1, 2, 3,, 24 depicts the total number of hour and *s* = 1, 2, 3,, 25 reveals the status of the switch of distributed sources.

2) CREATING INITIALIZATION CELL

After initialization of the random decimal and binary matrix, a cell is needed to form following the Eq. 3 and Eq. 4. After creating the cell, the best cell will be stored in *Pbest_TD* and *Pbest_TB* for the decimal and binary, respectively.

$$swarmT_{(1,k)} = \left\{ \begin{bmatrix} swarm_{(1,1)} & \cdots & swarm_{(1,s)} \\ \vdots & \ddots & \vdots \\ swarm_{(h,1)} & \cdots & swarm_{(h,s)} \end{bmatrix}_{(1,1)} \cdots \cdots \begin{bmatrix} swarm_{(1,1)} & \cdots & swarm_{(1,s)} \\ \vdots & \ddots & \vdots \\ swarm_{(h,1)} & \cdots & swarm_{(h,s)} \end{bmatrix}_{(1,k)} \right\} \quad (3)$$

TABLE 5. Pseudo code for internal loop with binary conversion.

```

for iteration from 1 to I do
    [fbest, best] = min(Evaluation)
    gbest = swarm_TD{best}
    for n from 1 to N do
        Find the value of v{k} according to equation (9)
        Evaluate the newpos following equation (10)
        Determining swarm_TD{k}
        for m from 1 to h do
            for j from 1 to s do
                Convert decimal to binary following equation (5)
            end
        end
    end
end
end
end
    
```

$$\begin{aligned}
 & swarmTB_{(1,k)} \\
 & = \left\{ \begin{array}{c} \left[\begin{array}{ccc} swarmB_{(1,1)} & \cdots & swarmB_{(1,s)} \\ \vdots & \ddots & \vdots \\ swarmB_{(h,1)} & \cdots & swarmB_{(h,s)} \end{array} \right]_{(1,1)} \cdots \cdots \\ \left[\begin{array}{ccc} swarmB_{(1,1)} & \cdots & swarmB_{(1,s)} \\ \vdots & \ddots & \vdots \\ swarmB_{(h,1)} & \cdots & swarmB_{(h,s)} \end{array} \right]_{(1,k)} \end{array} \right\} \quad (4)
 \end{aligned}$$

where, $swarmT$ is the total of all $swarm$ cells; $swarmTB$ is the total of all $swarmB$ cells; k is population size.

3) CONVERSION OF DECIMAL TO BINARY

The decimal cells are converted into binary cells following the sigmoid function shown in Eq. 5 and the conversion of 0 or 1 value is shown in Eq. 6.

$$\text{sigmoid}(T_{(i)}) = \frac{1}{1 + e^{-T_{(i)}}} \quad (5)$$

$$\begin{aligned}
 & \text{If } \text{sigmoid} > \text{rand then } TB_{(i)} = 1 \\
 & \text{else } TB_{(i)} = 0 \quad (6)
 \end{aligned}$$

4) INTERNAL LOOP

The iteration loop runs for 100 times with 20 particles swarm and each swarm carrying a schedule of 600 values. Table 5 reflects the pseudo code for internal loop with binary conversion using sigmoid function. The minimum evaluation will be stored at $fbest$ and it location $best$. Also $swarm_TDbest$ will be saved to $gbest$ as in Eq. 7 and Eq. 8.

$$[fbest, best] = \min(Evaluation) \quad (7)$$

$$gbest = swarm_TDbest \quad (8)$$

Throughout the search process, the velocity and position of each swarm can be updated according to Eq. 9 and Eq. 10.

$$\begin{aligned}
 v\{k\} &= w * v\{k\} + c1 * rand * (Pbest_TD\{k\} \\
 &\quad - swarm_TD\{k\}) + c2 * rand \\
 &\quad * (gbest - swarm_TD\{k\}) \quad (9)
 \end{aligned}$$

TABLE 6. Pseudo code for evaluating the fitness function.

```

Conditions
Set weather, price and grid status conditions in total binary positions
TB {i}(m,j)
swarmB = swarm_TB{k}
Run Simulink ( TB {i}(m,j) ) and
Finding the fitness function according to equation (11)

newpos = swarmTDk + v{k}
swarm\_TDk = new\_pos \quad (10)
    
```

Afterward, the simulation runs with the current cell to provide the system with binary matrix. Therefore, condition zero and one reflect the specific DG will be Off ON, respectively. Table 6 depicts the pseudo code for finding the fitness function. The target of this research is to minimize the carbon emission and energy consumption of the existing power network by replacing the power coming from national grid with small-distributed generations. In this research, BPSO is designed to be a global minimizer and selecting minimum fitness with global minimum for finding the best cell by calculating objective function in equation (11) and compare to previous best Cell at every iteration. Thus, the fitness function in this process is the mean cost to obtain the minimum desired outcome as in Eq. 11.

$$MC = \left(\frac{3}{2}\right) IV * p.f. * RM / KWh \quad (11)$$

where, I and V denote the total current and voltage; $p.f.$ reflects the power factor; RM/KWh reveals the energy pricing per hour. Here, in the grid, the power factor is chosen 0.85. As the DGs inject the real power only at unity power factor, the overall power factor should reduce from 0.85. To control this poor power factor, inverter with reactive power control is used which can convert the dc power to ac, and at the same time can reduce the both active and reactive power from the grid to make the power factor stable. Thus, to obtain the desired objective function, the following constraints have been followed,

$$\begin{aligned}
 & V_{w,cut-in} = 0.5ms^{-1} \\
 & Irradiance_{solar} \geq 50watt/m^2 \\
 & P_g^{net} (grid) + P_g^{net} (DGs) \geq P_{load}^{net} \quad (12)
 \end{aligned}$$

5) BEST CELL

The objective is to minimize the MC to minimum at the end of the optimization and the minimum evaluation will have a location in the memory following Table 7. Thus the best schedule is obtained according to Eq.13 and Eq. 14.

$$[x, y] = \min (Evaluation) \quad (13)$$

$$Best_{sch} = Pbest_{TB\{y\}} \quad (14)$$

The BPSO operational algorithm is shown in Fig. 7.

TABLE 7. Pseudo code for the best schedule.

```

for n from 1 to N do
  if MC < Evaluation(k)
  then Pbest_TD{k} = swarm_TD{k}
       Pbest_TB{k} = swarm_TB{k}
       Evaluation(k) = MC end
end
objective(i) = min(Evaluation)
Finding the location
end
Finding the best schedule
  
```

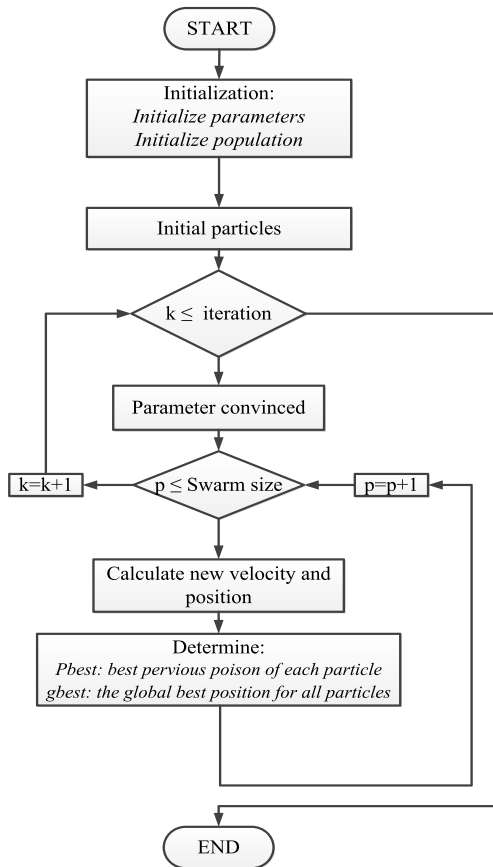


FIGURE 7. BPSO optimization algorithms operational flow.

V. RESULTS AND DISCUSSION

The obtained results of the proposed BPSO optimization algorithm are validated in terms of objective function, scheduling controller and optimal energy generation under different conditions. The result shows how the optimized algorithm in the VPP and MG can reduce the power in order to reduce the consumption and increase the profit. Energy consumption, and the electricity cost are calculated following the equations below:

$$E_{kWh/day} = P(kW) \times t_h/day \tag{15}$$

$$Cost_{RM/day} = \frac{E_{kwh/day} \times Cost_{cent/kWh}}{100_{cent/RM}} \tag{16}$$

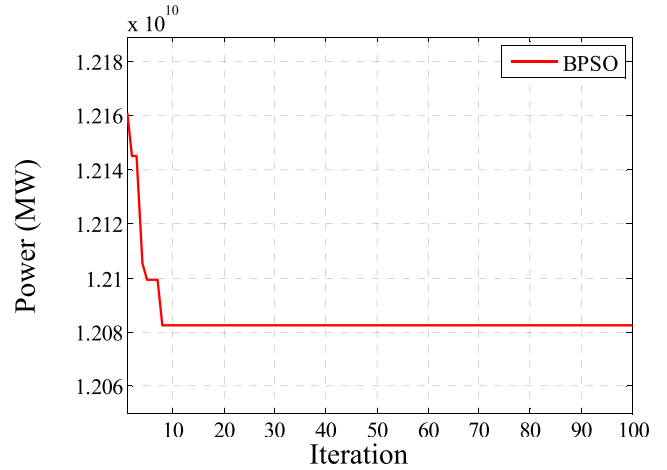


FIGURE 8. Optimization objective for BPSO.

To obtain the results, IEEE 14 bus system including the real data in the VPP runs hundred times for several days to achieve the best objective function in order to develop the best scheduling controller to reduce the power consumption and carbon emission, respectively. Fig. 8 shows the optimization of the objection function of 100 iterations using BPSO. It is also seen that the function is converge shortly and reduced the huge amount of power consumption, which is almost impossible in trial and error methods.

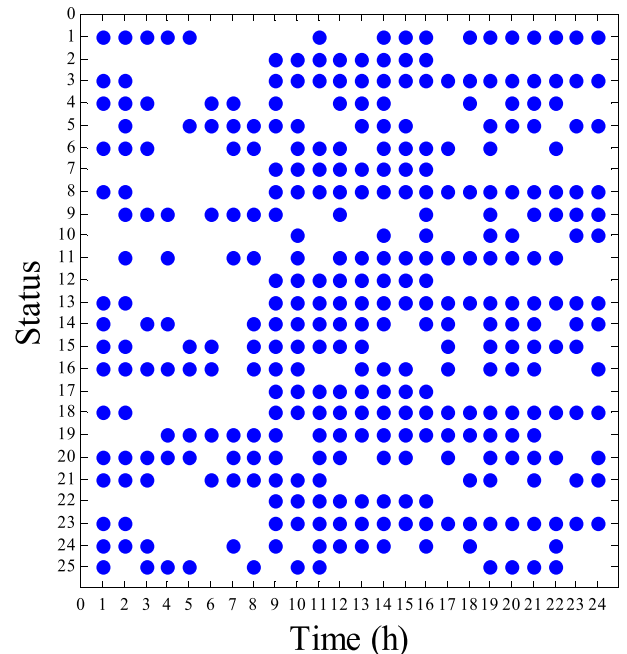


FIGURE 9. Spy figure for the best schedule for BPSO.

BPSO optimization algorithm generates binary decision of 0 and 1 for the scheduling controller; where 0 represents OFF state and 1 represent ON state for the individual DG at any specific hour in the EMS schedule. This operation took 4000 tries for initializations and iterations of the controller to obtain the best schedule for the operation. Fig. 9 shows

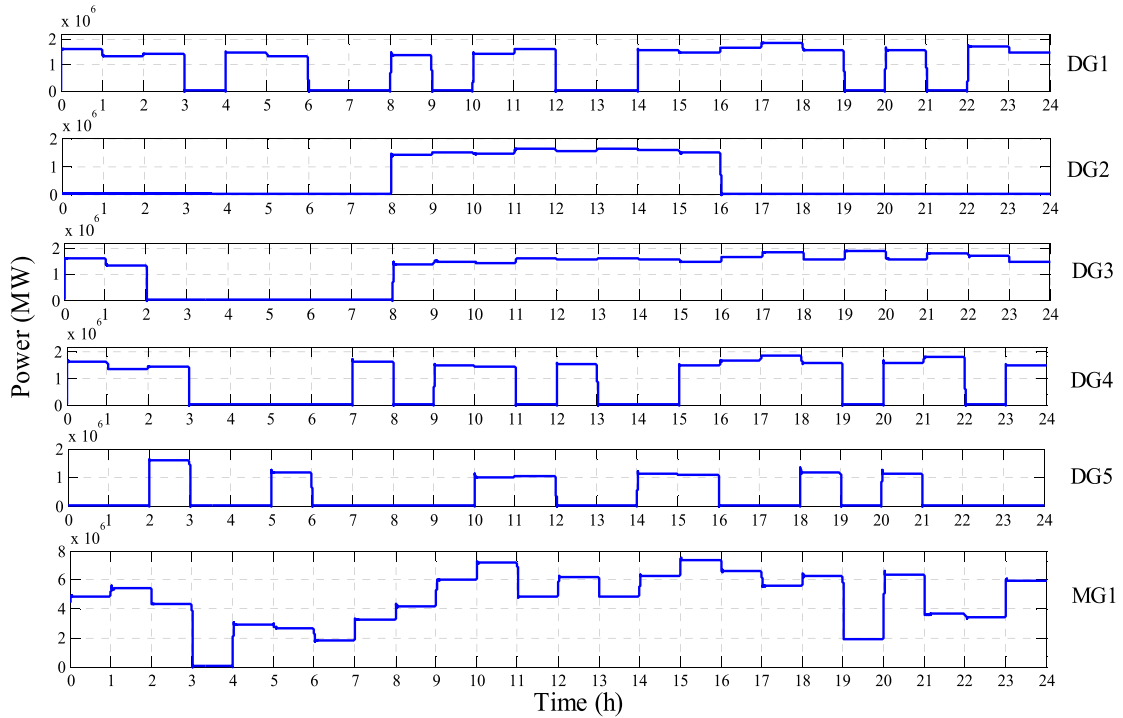


FIGURE 10. RESs and MG power for MG1 at bus 5 using BPSO.

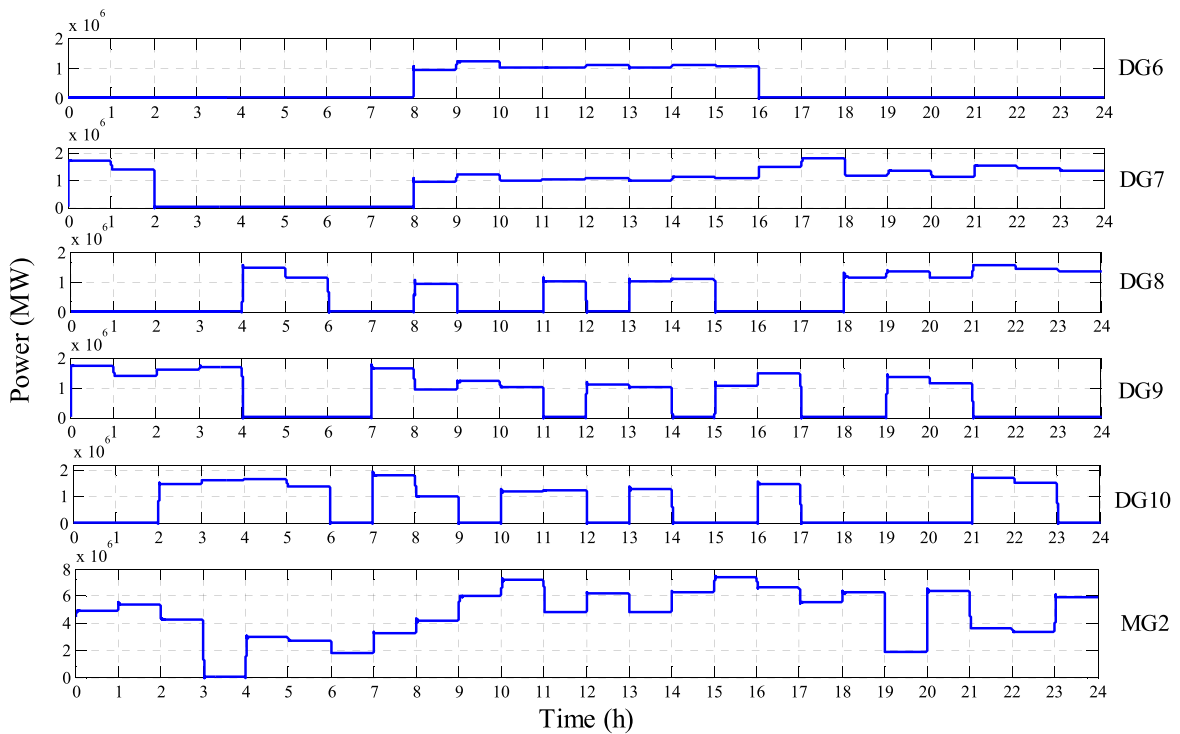


FIGURE 11. RESs and MG power for MG2 at bus 6 using BPSO.

the ON and OFF states for 24 hours of operation for the best schedule using BPSO. This ON and OFF schedule of the DGs are based on the conditions of weather data, battery charge/discharges and fuel states, respectively.

A. EXPERIMENTAL SETUP

Testing of this system is based on the experimental setup to show the participation of the MG and its sources in case of BPSO algorithm. The system includes five MGs

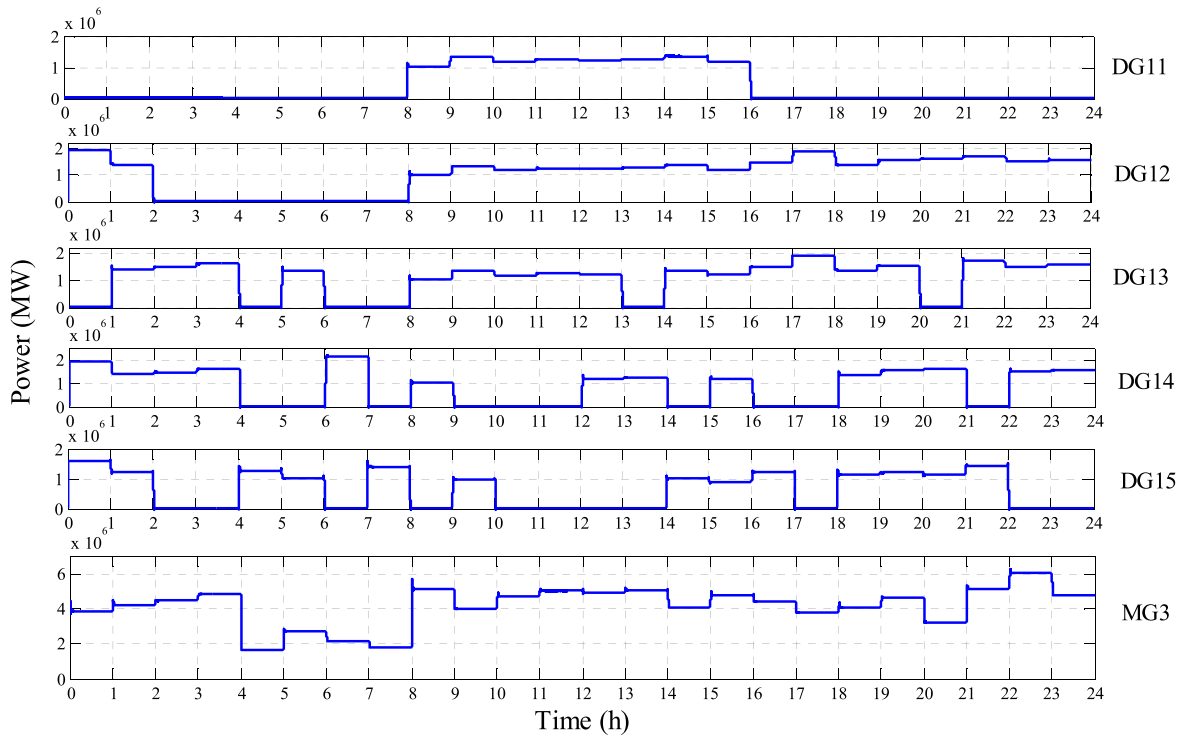


FIGURE 12. RESs and MG power for MG3 at bus10 using BPSO.

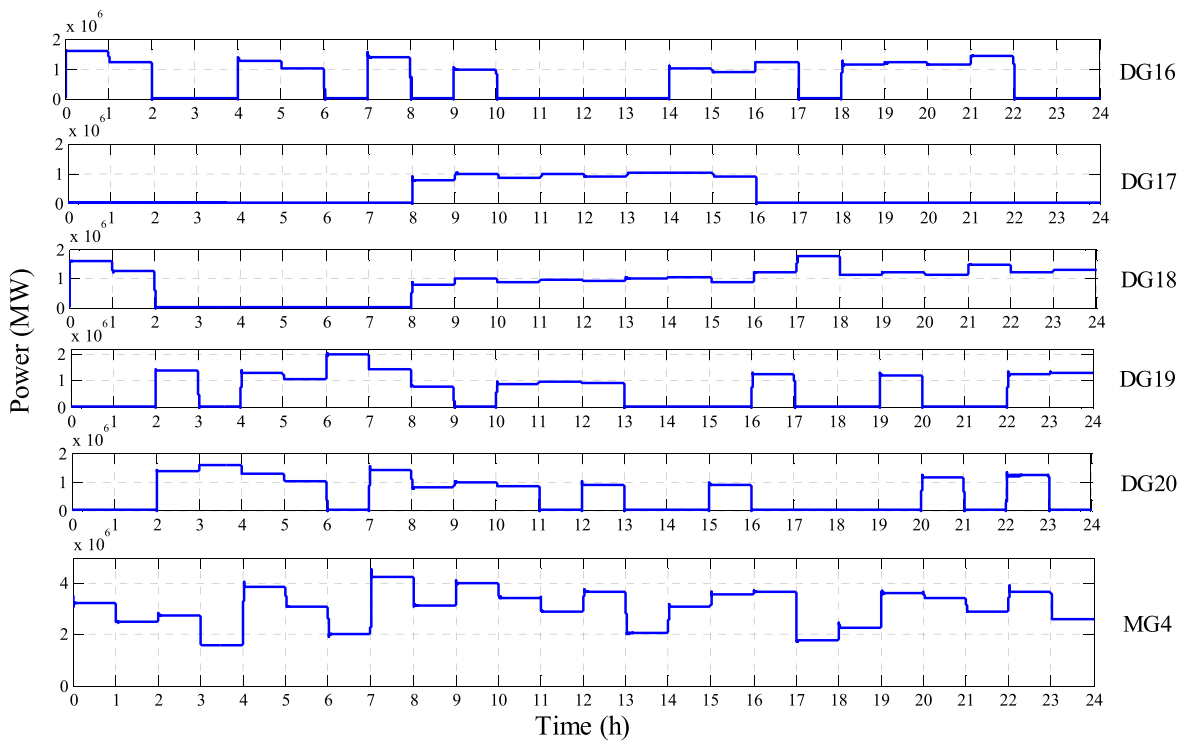


FIGURE 13. RESs and MG power for MG4 at bus11 using BPSO.

each MG includes five DGs, so the numbering of the DG starts with DG1 end to DG25 as a results DG1 to DG5 at MG1, DG6 to DG10 at MG2, DG11 to DG15 at MG3,

DG16 to DG20 at MG4, and DG21 to DG25 at MG5, respectively. Table 8 represents each DG numbers, types and capacity.

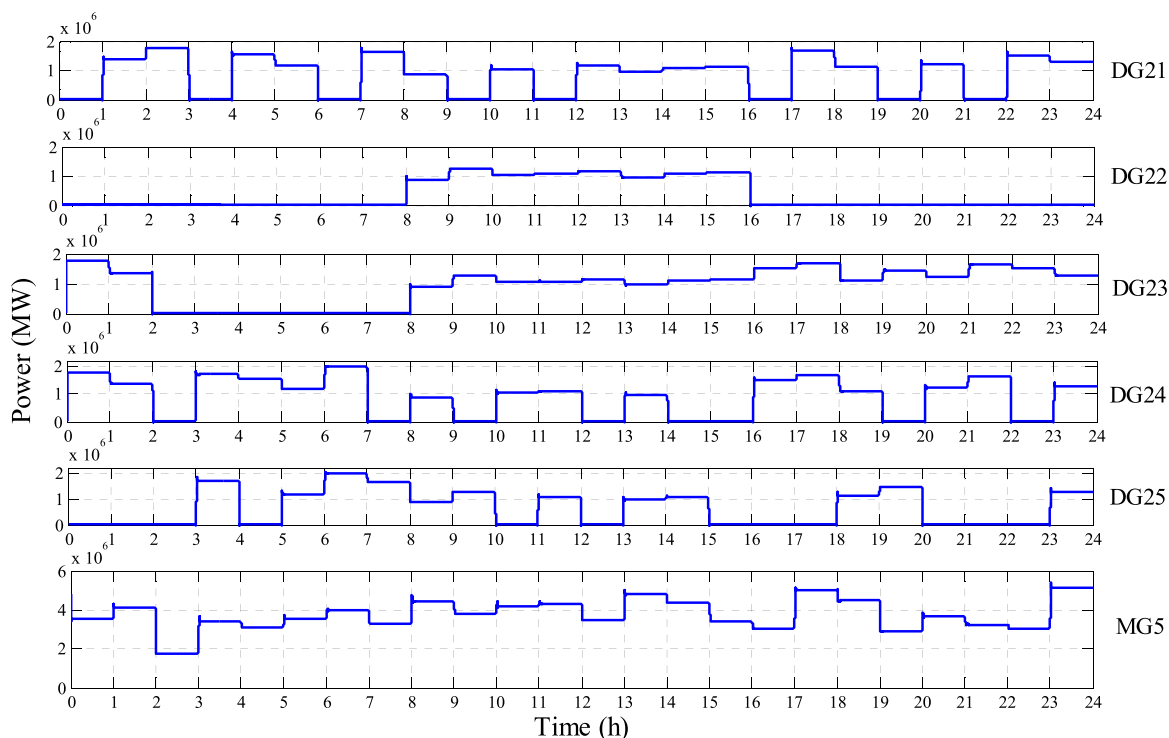


FIGURE 14. RESs and MG power for MG5 at bus13 using BPSO.

TABLE 8. Distributed generation types and capacities.

Distributed Generator	DG Capacity	Source type
DG1, DG6, DG11, DG16, DG21	20 MW	Diesel generator
DG2, DG7, DG12, DG17, DG22	10 MW	Photovoltaic
DG3, DG8, DG13, DG18, DG23	10 MW	Wind turbine
DG4, DG9, DG14, DG19, DG24	5 MW	Fuel cell (SOFC)
DG5, DG10, DG15, DG20, DG25	5 MW	Battery

This system runs for one day with hourly real time variable data, so that the algorithm in each change enables the renewable sources to supply the power to the load depending on the availability of distribution generations throughout the operation.

B. BPSO ALGORITHM TEST

The best schedule is obtained by applying BPSO on the IEEE 14 bus system with MGs and their RESs. This test shows the characteristics of each source in every MG in terms of ON and OFF using BPSO algorithm as shown in Fig. 10 to Fig. 14, following from MG1 to MG5 at bus 5, bus 6, bus 10, bus 11 and bus 13, respectively. From the analysis, it is seen that, each source of every MG gives separate power at different times of the day; therefore the total power also varies at different buses throughout the day which has been shown at the last signal in each figure. It is also seen that BPSO

optimization algorithm find the best schedule to connect the RESs and MGs in the VPP and the grid based on the constraint of the objective function.

In Fig.15, a comparative study has been conducted to show the effectiveness of the developed BPSO algorithm in which the main grid power at bus 1 is compared with no grid connection, random schedule and BPSO optimized schedule, respectively. The power drawing from the main grid is extremely reduces when BPSO optimized MGs are installed which is approximately 47% power saving for the national grid compared to with MGs. Accordingly, it will be easy to generate reduced power to fulfill the demand and keep the generation margin between generation and consumption. Fig. 16 shows the power saved using BPSO algorithm. Following the eq. 16, the total cost saved with BPSO is RM 232124.5674.

C. CO₂ EMISSION REDUCTION

In general, CO₂ emissions are estimated using the information on fuel consumption in units and heat content of fuel in MMBtu multiplied by specific emission factor [32]. However, an emission per kWh is used with power quality data relating to electricity efficiencies [45].

According to the Intergovernmental Panel on Climate Change (IPCC), the world emits approximately 27 gigatonnes of CO₂ e from multiple sources and with electrical production emitting 10 gigatonnes which approximately 37% of global emissions [46]. Electricity consumption is one of the largest sources of carbon emissions. Thus, it is essential to measure

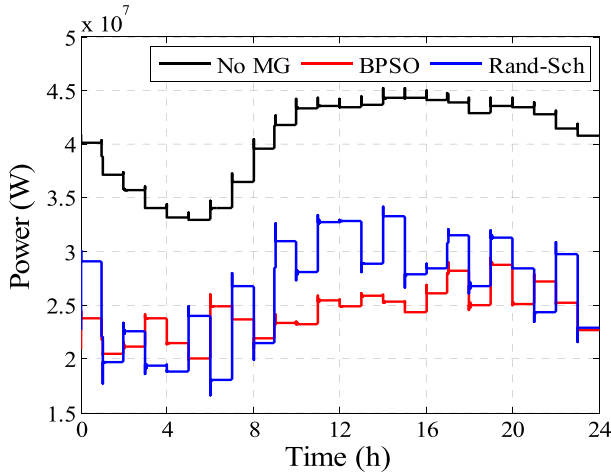


FIGURE 15. Main grid power at Bus1 supply to the IEEE 14 bus system with and without MGs connected.

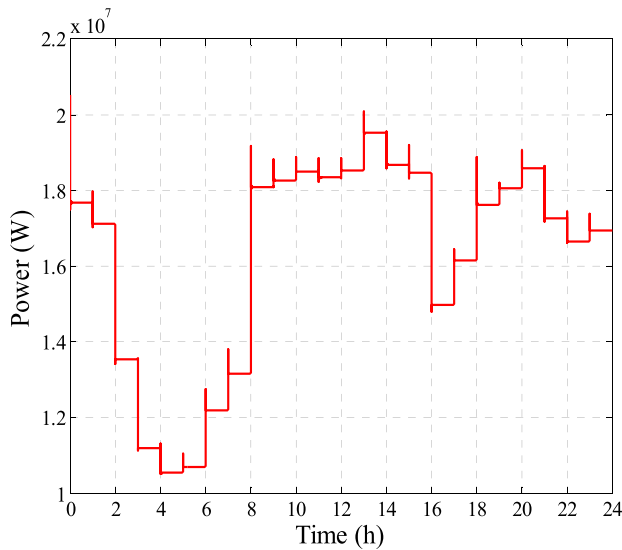


FIGURE 16. Power saved when applying BPSO schedule controller.

carbon emissions perfectly. The carbon emission calculation depends on some factors such as electricity consumption, composite electricity or heat emission factors, respectively. These factors are varying from country to country. Based on International Energy Agency (IEA), composite electricity/heat factors in Malaysia is 0.6559169 kgCO₂/kWh. To be more specific, the electricity specific factors in Malaysia is 0.74884244 kgCO₂/kWh [47]. In this study, CO₂ emissions of power consumption are calculated by applying an emission factor (EF) to the amount of kilowatt hours (kWh) consumed by VPP as in Eq. 17.

$$kWh \times EF = GHG (kgCO_2) \quad (17)$$

where, GHG is greenhouse gases, EF is the emission factor, and kWh is the amount of power consumed by VPP. Fig. 17 shows that amount of CO₂ emission reduction is

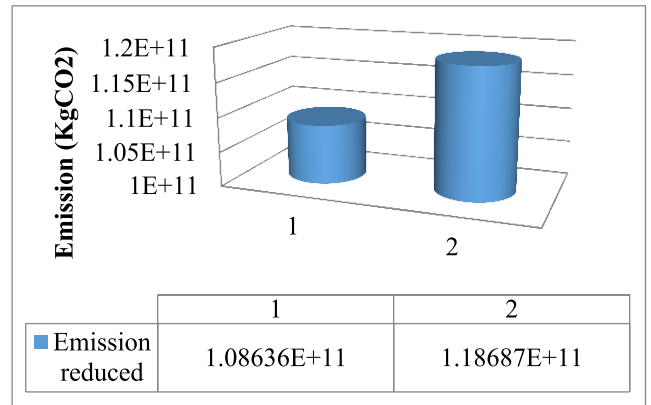


FIGURE 17. Comparison of GHG emission reduction using 1) BPSO scheduling controller 2) random scheduling controller.

higher using BPSO algorithm based schedule controller compare to random schedule controller.

The proposed model has been compared with other proposed algorithm by different researchers for testing the performance in saving the energy and costs. Comparative analysis among the researches is shown below:

TABLE 9. Comparative analysis of proposed model with other models.

Algorithm	Power saving (%)	Cost saving	Emission reduction (%)	Computational time (minute)	Ref.
BPSO	47%	2.72%	8.46%	2880	Proposed
BBSA	45%	2.60%	8.1%	4220	[29]
GA	--	0.1 – 0.33%	--	--	[48]
Stochastic linear programming model	32.73 – 42.67%	2.34%	15.17%	--	[49]
Immune algorithm	--	1.52%	4.48%	--	[50]

From the analysis, it is seen that, BPSO performs satisfactorily in saving power, costs and emission reduction. Moreover, it requires less computational time as it has less parameters as constraints.

VI. CONCLUSION

MGs in a real system could surely reduce the energy consumptions; however, RESs in the MGs need a robust controller to organize their work efficiently. Accordingly, the objective of this study is achieved in developing a novel BPSO algorithm based scheduling controller for the energy management system of an IEEE14 bus system which includes multi MGs integrated with RESs to form virtual power plant. The VPP system is modeled and simulated with real data of load recorded in February 2016 at Perlis, Malaysia. The developed BPSO algorithm resulted in an optimal scheduling control for the sustainable energy utilization of the VPP with

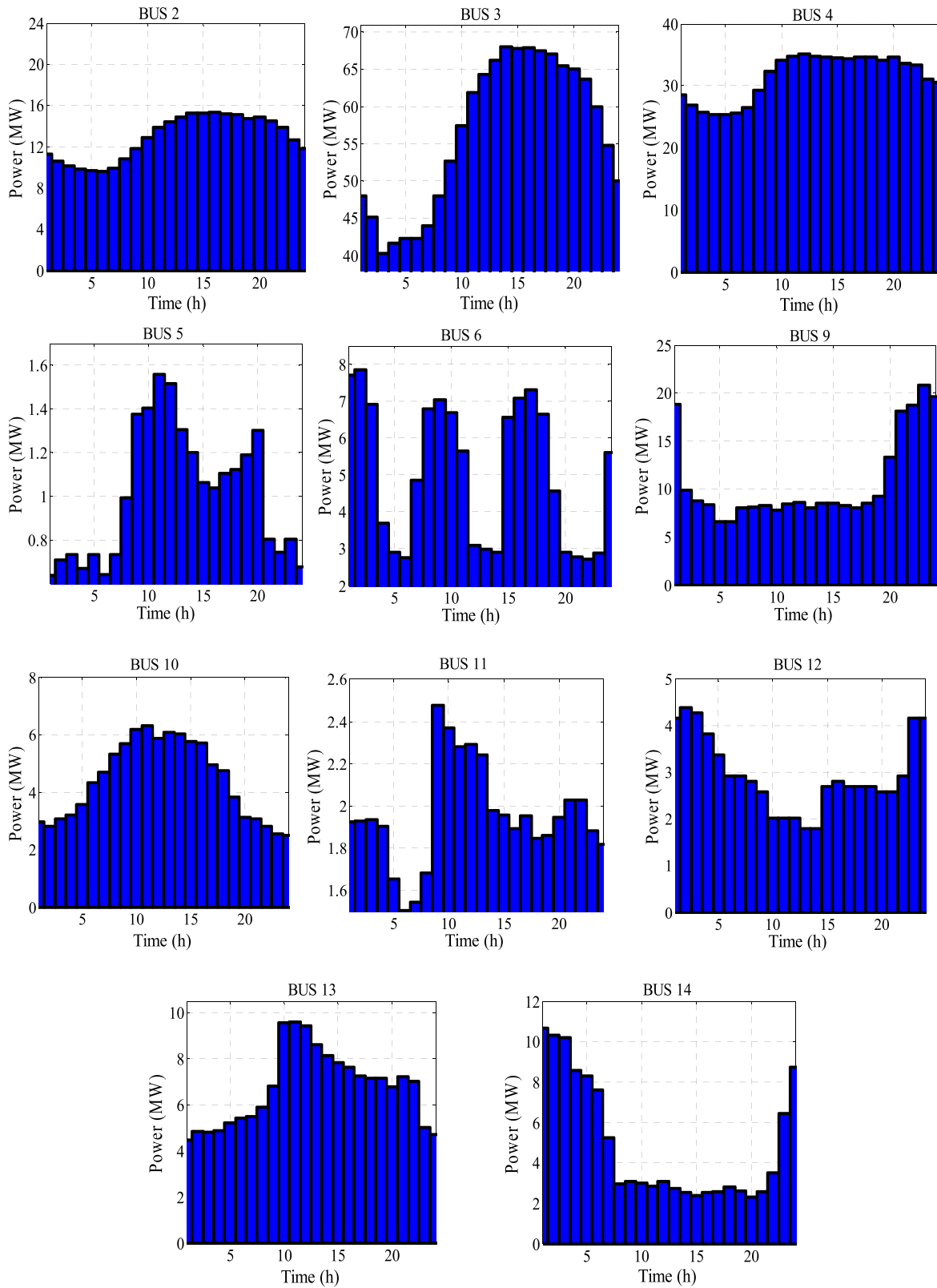


FIGURE 18. Load curve in MW for each load in IEEE 14 bus test system.

RESs integrated MGs. Obtained results show the significant contribution to reduce 47% grid energy consumption and reduce the CO₂ emission by 8.46% compare with random

scheduling controller. Compare with other algorithm and controller also, BPSO shows better performance in power saving, cost saving and emission reduction. Moreover, BPSO

requires less computational time. Overall, the optimal BPSO algorithms give priority in selection ON and OFF of the RES schedule depend on the RES importance, per unit cost and availability to cover the demand. Compassion among the algorithms shows that the BPSO algorithm outperforms other non-optimized or optimized controllers in terms of consumption reduction, energy and cost saving and carbon reduction which in turns validate the development.

APPENDIX

See Fig. 18.

REFERENCES

- [1] Q. Wang, F. Zhao, and T. Chen, "A base station DTX scheme for OFDMA cellular networks powered by the smart grid," *IEEE Access*, vol. 6, pp. 63442–63451, 2018.
- [2] A. Kuriyama and N. Abe, "Ex-post assessment of the Kyoto Protocol—Quantification of CO₂ mitigation impact in both Annex B and non-Annex B countries—," *Appl. Energy*, vol. 220, pp. 286–295, Jun. 2018.
- [3] K. Vaillancourt, O. Bahn, E. Frenette, and O. Sigvaldason, "Exploring deep decarbonization pathways to 2050 for Canada using an optimization energy model framework," *Appl. Energy*, vol. 195, pp. 774–785, Jun. 2017.
- [4] F. J. D. Perez, M. R. P. Otin, A. G. Mouhaffel, R. D. Martin, and D. Chinarro, "Energy and water consumption and carbon footprint in tourist pools supplied by desalination plants: Case study, the canary islands," *IEEE Access*, vol. 6, pp. 11727–11737, 2018.
- [5] U. Akram, M. Khalid, and S. Shafiq, "An improved optimal sizing methodology for future autonomous residential smart power systems," *IEEE Access*, vol. 6, pp. 5986–6000, 2018.
- [6] K. A. Babatunde, R. A. Begum, and F. F. Said, "Application of computable general equilibrium (CGE) to climate change mitigation policy: A systematic review," *Renew. Sustain. Energy Rev.*, vol. 78, pp. 61–71, Oct. 2017.
- [7] R. Ara, K. Sohag, S. Mastura, S. Abdullah, and M. Jaafar, "CO₂ emissions, energy consumption, economic and population growth in Malaysia," *Renew. Sustain. Energy Rev.*, vol. 41, pp. 594–601, Jan. 2015.
- [8] N. S. M. Safaai, Z. Z. Noor, H. Hashim, Z. Ujang, and J. Talib, "Projection of CO₂ emissions in malaysia," *Environ. Prog. Sustain. Energy*, vol. 30, no. 4, pp. 658–665, 2011.
- [9] F. Birol, "CO₂ emissions from fuel combustion," OECD/IEA, Int. Energy Agency, Paris, France, 2017.
- [10] M. Faisal, M. A. Hannan, P. J. Ker, A. Hussain, M. B. Mansor, and F. Blaabjerg, "Review of energy storage system technologies in microgrid applications: Issues and challenges," *IEEE Access*, vol. 6, pp. 35143–35164, 2018.
- [11] M. H. Andishgar, E. Gholipour, and R.-A. Hooshmand, "An overview of control approaches of inverter-based microgrids in islanding mode of operation," *Renew. Sustain. Energy Rev.*, vol. 80, pp. 1043–1060, Dec. 2017.
- [12] A. A. K. Arania, H. Karamia, G. B. Gharehpetiana, and M. S. A. Hejazi, "Review of Flywheel Energy Storage Systems structures and applications in power systems and microgrids," *Renew. Sustain. Energy Rev.*, vol. 69, pp. 9–18, Mar. 2017.
- [13] H. Lan, S. Wen, Y.-Y. Hong, D. C. Yu, and L. Zhang, "Optimal sizing of hybrid PV/diesel/battery in ship power system," *Appl. Energy*, vol. 158, pp. 26–34, Nov. 2015.
- [14] U. Akram, M. Khalid, and S. Shafiq, "An innovative hybrid wind-solar and battery-supercapacitor microgrid system—Development and optimization," *IEEE Access*, vol. 5, pp. 25897–25912, 2017.
- [15] M. Jain, S. Gupta, D. Masand, G. Agnihotri, and S. Jain, "Real-time implementation of islanded microgrid for remote areas," *J. Control Sci. Eng.*, vol. 2016, Feb. 2016, Art. no. 5710950. doi: [10.1155/2016/5710950](https://doi.org/10.1155/2016/5710950).
- [16] M. F. Roslan, M. A. Hannan, P. Jern, and M. N. Uddin, "Microgrid control methods toward achieving sustainable energy management," *Appl. Energy*, vol. 240, pp. 583–607, Apr. 2019.
- [17] G. Liu, T. Jiang, T. B. Ollis, X. Zhang, and K. Tomsovic, "Distributed energy management for community microgrids considering network operational constraints and building thermal dynamics," *Appl. Energy*, vol. 239, pp. 83–95, Apr. 2019.
- [18] D. Koraki and K. Strunz, "Wind and solar power integration in electricity markets and distribution networks through service-centric virtual power plants," *IEEE Trans. Power Syst.*, vol. 33, no. 1, pp. 473–485, Jan. 2018.
- [19] A. Baringo, L. Baringo, and J. M. Arroyo, "Day-ahead self-scheduling of a virtual power plant in energy and reserve electricity markets under uncertainty," *IEEE Trans. Power Syst.*, vol. 34, no. 3, pp. 1881–1894, May 2019.
- [20] D. Arcos-Aviles, J. Pascual, L. Marroyo, P. Sanchis, and F. Guinjoan, "Fuzzy logic-based energy management system design for residential grid-connected microgrids," *IEEE Trans. Smart Grid*, vol. 9, no. 2, pp. 530–543, Mar. 2018.
- [21] J. Reynolds, M. W. Ahmad, Y. Rezgui, and J.-L. Hippolyte, "Operational supply and demand optimisation of a multi-vector district energy system using artificial neural networks and a genetic algorithm," *Appl. Energy*, vol. 235, pp. 699–713, Feb. 2019.
- [22] X. Zhang, Y. Chen, T. Yu, B. Yang, K. Qu, and S. Mao, "Equilibrium-inspired multiagent optimizer with extreme transfer learning for decentralized optimal carbon-energy combined-flow of large-scale power systems," *Appl. Energy*, vol. 189, pp. 157–176, Mar. 2017.
- [23] P. Moutis, P. S. Georgilakis, and N. D. Hatziargyriou, "Voltage regulation support along a distribution line by a virtual power plant based on a center of mass load modeling," *IEEE Trans. Smart Grid*, vol. 9, no. 4, pp. 3029–3038, Jul. 2018.
- [24] M. Javidsharifi, T. Niknam, J. Aghaei, and G. Mokryani, "Multi-objective short-term scheduling of a renewable-based microgrid in the presence of tidal resources and storage devices," *Appl. Energy*, vol. 216, pp. 367–381, Apr. 2018.
- [25] S. M. A. Elazim and E. S. Ali, "Optimal SSSC design for damping power systems oscillations via Gravitational Search Algorithm," *Int. J. Electr. Power Energy Syst.*, vol. 82, pp. 161–168, Nov. 2016.
- [26] H. Shareef, A. A. Ibrahim, and A. H. Mutlag, "Lightning search algorithm," *Appl. Soft Comput. J.*, vol. 36, pp. 315–333, Nov. 2015.
- [27] M. A. Hannan, J. A. Ali, A. Mohamed, U. A. U. Amirulddin, N. M. L. Tan, and M. N. Uddin, "Quantum-behaved lightning search algorithm to improve indirect field-oriented fuzzy-PI control for IM drive," *IEEE Trans. Ind. Appl.*, vol. 54, no. 4, pp. 3793–3805, Jul./Aug. 2018.
- [28] G. Comodi, A. Giantomassi, M. Severini, S. Squartini, F. Ferracuti, A. Fonti, D. N. Cesarini, M. Morodo, and F. Polonara, "Multi-apartment residential microgrid with electrical and thermal storage devices: Experimental analysis and simulation of energy management strategies," *Appl. Energy*, vol. 137, pp. 854–866, 2015.
- [29] M. G. M. Abdolrasol, M. A. Hannan, A. Mohamed, U. A. U. Amirulddin, I. B. Z. Abidin, and M. N. Uddin, "An optimal scheduling controller for virtual power plant and microgrid integration using the binary backtracking search algorithm," *IEEE Trans. Ind. Appl.*, vol. 54, no. 3, pp. 2834–2844, May/Jun. 2018.
- [30] A. Rabiee, M. Sadeghi, J. Aghaei, and A. Heidari, "Optimal operation of microgrids through simultaneous scheduling of electrical vehicles and responsive loads considering wind and PV units uncertainties," *Renew. Sustain. Energy Rev.*, vol. 57, pp. 721–739, May 2016.
- [31] H. Kamankesh, V. G. Agelidis, and A. Kavousi-Fard, "Optimal scheduling of renewable micro-grids considering plug-in hybrid electric vehicle charging demand," *Energy*, vol. 100, pp. 285–297, Apr. 2016.
- [32] F. Najibi and T. Niknam, "Stochastic scheduling of renewable micro-grids considering photovoltaic source uncertainties," *Energy Convers. Manage.*, vol. 98, pp. 484–499, Jul. 2015.
- [33] S. Yu, F. Fang, Y. Liu, and J. Liu, "Uncertainties of virtual power plant: Problems and countermeasures," *Appl. Energy*, vol. 239, pp. 454–470, Apr. 2019.
- [34] C. Wei, J. Xu, S. Liao, Y. Sun, Y. Jiang, D. Ke, Z. Zhang, and J. Wang, "A bi-level scheduling model for virtual power plants with aggregated thermostatically controlled loads and renewable energy," *Appl. Energy*, vol. 224, pp. 659–670, Aug. 2018.
- [35] T. Kerdpol, Y. Qudaih, and Y. Mitani, "Optimum battery energy storage system using PSO considering dynamic demand response for microgrids," *Int. J. Electr. Power Energy Syst.*, vol. 83, pp. 58–66, Dec. 2016.
- [36] M. Shabanzadeh, M.-R. Haghifam, and M.-K. Sheikh-El-Eslami, "An interactive cooperation model for neighboring virtual power plants," *Appl. Energy*, vol. 200, pp. 273–289, Aug. 2017.

- [37] S. Rahmani-dabbagh and M. K. Sheikh-El-Eslami, "A profit sharing scheme for distributed energy resources integrated into a virtual power plant," *Appl. Energy*, vol. 184, pp. 313–328, Dec. 2016.
- [38] H. Cui, F. Li, Q. Hu, L. Bai, and X. Fang, "Day-ahead coordinated operation of utility-scale electricity and natural gas networks considering demand response based virtual power plants," *Appl. Energy*, vol. 176, pp. 183–195, Aug. 2016.
- [39] V. Mohan, J. G. Singh, W. Ongsakul, and M. P. R. Suresh, "Performance enhancement of online energy scheduling in a radial utility distribution microgrid," *Int. J. Elect. Power Energy Syst.*, vol. 79, pp. 98–107, Jul. 2016.
- [40] T. Basso, "IEEE 1547 and 2030 standards for distributed energy resources interconnection and interoperability with the electricity grid," NREL, Lakewood, CO, USA, Tech. Rep. NREL/TP-5D00-63157, 2014.
- [41] T. Basso and R. DeBlasio, "IEEE smart grid series of standards IEEE 2030 (interoperability) and IEEE 1547 (interconnection) status," Nat. Renew. Energy Lab., Phoenix, AZ, USA, Tech. Rep. NREL/CP-5500-53028, 2011.
- [42] K. E. Martin *et al.*, "An overview of the IEEE standard C37.118.2—Synchrophasor data transfer for power systems," *IEEE Trans. Smart Grid*, vol. 5, no. 4, pp. 1980–1984, Jul. 2014.
- [43] Y. Zhou, C. Wang, J. Wu, J. Wang, M. Cheng, and G. Li, "Optimal scheduling of aggregated thermostatically controlled loads with renewable generation in the intraday electricity market," *Appl. Energy*, vol. 188, pp. 456–465, Feb. 2017.
- [44] H. G. G. Nunes, J. A. N. Pombo, S. J. P. S. Mariano, M. R. A. Calado, and J. A. M. F. de Souza, "A new high performance method for determining the parameters of PV cells and modules based on guaranteed convergence particle swarm optimization," *Appl. Energy*, vol. 211, pp. 774–791, Feb. 2018.
- [45] J. Yiyi and F. Kiyoshi, "Modeling the cost transmission mechanism of the emission trading scheme in China," *Appl. Energy*, vol. 236, pp. 172–182, Feb. 2019.
- [46] V. Masson-Delmotte *et al.*, "Summary for policymakers. In: Global warming of 1.5 °C. An IPCC Special Report on the impacts of global warming of 1.5 °C above pre-industrial levels and related global greenhouse gas emission pathways, in the context of strengthening the global response to the threat of climate change, sustainable development, and efforts to eradicate poverty," Inter-Governmental Panel Climate Change, Geneva, Switzerland, 2018.
- [47] A. M. Brander, A. Sood, C. Wylie, A. Haughton, and J. Lovell, "Electricity-specific emission factors for grid electricity," *Econometrica*, Edinburgh, U.K., 2011, pp. 1–22.
- [48] Q. Ai, S. Fan, and L. Piao, "Optimal scheduling strategy for virtual power plants based on credibility theory," *Protection Control Mod. Power Syst.*, vol. 1, no. 1, p. 3, Dec. 2016.
- [49] C. Zhou, G. Huang, and J. Chen, "Planning of electric power systems considering virtual power plants with dispatchable loads included: An inexact two-stage stochastic linear programming model," *Math. Problems Eng.*, vol. 2018, Aug. 2018, Art. no. 7049329. doi: 10.1155/2018/7049329.
- [50] W. Hua, D. Li, H. Sun, P. Matthews, and F. Meng, "Stochastic environmental and economic dispatch of power systems with virtual power plant in energy and reserve markets," *Int. J. Smart Grid Clean Energy*, vol. 7, no. 4, pp. 231–239, 2018.

• • •